Int. J. Heat Mass Transfer. Vol. 13, pp. 1887–1905. Pergamon Press 1970. Printed in Great Britain

MASS TRANSFER OF DECAYING PRODUCTS WITH AXIAL DIFFUSION IN CYLINDRICAL TUBES†

C. W. TAN
The Cooper Union for the Advancement of Science and Art, New York, N.Y., U.S.A.

and

CHIA-JUNG HSU
Brookhaven National Laboratory, Upton, N.Y., U.S.A.

(*Received* 29 *December* 1969 *and in revised form* 31 *March* 1970)

Abstract—The problem of steady-state mass transfer with axial diffusion of decaying products resulting from the disintegration of an inert gas is considered for a slug and a Poiseuille pipe flow. The products of disintegration are filtered out at the tube inlet, but are again generated by radioactive decay of a flowing inert gas along the cylindrical tube. The radio-elements diffuse axially and radially to the tube walls where they decay into other radio-elements.

Because of the Péclét number dependence, the effects of the axial diffusion on the concentration distribution, the local Sherwood number, and the $F(\xi)$ values are studied for Péclét numbers of 1, 5, 10, 20, 30, 50, 100 and ∞.

For the Poiseuille pipe flow, asymptotic expressions for the eigenvalues and the eigenfunctions are also obtained.

NOMENCLATURE

A_n, coefficients of series expansion in equation (7);
c, mass concentration of the decaying product;
c_b, local bulk concentration, defined as $\int_0^{r_0} v_x cr\,\mathrm{d}r / \int_0^{r_0} v_x r\,\mathrm{d}r$;
c_f, fully established mass concentration;
c^*, defined as $c - c_f$;
C_n, coefficients of series expansion in equation (15);
D, coefficient of diffusion;
$F_f(\xi)$, defined as $2\pi \int_0^{r_0} v_x cr\,\mathrm{d}r/\pi r_0^2 xq$;
$F_f^*(\xi)$, defined as $2\pi \int_0^{r_0} (v_x c - D\partial c/\partial x) \times r\,\mathrm{d}r/\pi r_0^2 xq$;
I, mass flux density;
Pe, Péclét number of diffusion, defined as $ReSc = (2Vr_0/D)$;
$P_n(\eta)$, eigenfunctions for equations (8) and (9);
q, rate of formation of the decaying product per unit volume of gas;
r, radial coordinate distance;
r_0, inner radius of the tube;
$R_n(\eta)$, eigenfunctions for equations (16) and (17);
Sh, Sherwood number, defined as $h_D(2r_0)/D$;
v_x, v_r, axial and radial velocity components, respectively;
V, mean flow velocity;
x, axial coordinate distance;

† This work was performed under the auspices of the U.S. Atomic Energy Commission.

α_n, eigenvalues of equations (8) and (9), such that $\alpha_n^2 = \lambda_n^2[1 + (2\lambda_n/Pe)^2]$;
β_n, eigenvalues of equations (16) and (17);
λ_n, eigenvalues of equations (8) and (9);
η, defined as r/r_0;
ξ, defined as $x/(r_0 ReSc)$;
μ, defined as $2x/(r_0 ReSc) = 2\xi$;
ψ, dimensionless mass concentration, defined as Dc/qr_0^2;
ψ^*, defined as Dc^*/qr_0^2;
ψ_b, defined as Dc_b/qr_0^2;
Λ_x, Λ_r, dimensionless axial and radial velocity components, defined as v_x/V and v_r/V, respectively.

INTRODUCTION

THE PROBLEM of steady-state mass diffusion of a constituent in a generating but nonreacting binary gas mixture flowing through a cylindrical tube, assuming azimuthal symmetry and constant coefficient of diffusion can be written mathematically as [1]:

$$v_x \frac{\partial c}{\partial x} + v_r \frac{\partial c}{\partial r} = D\left[\frac{1}{r}\frac{\partial}{\partial r}\left(r\frac{\partial c}{\partial r}\right) + \frac{\partial^2 c}{\partial x^2}\right] + q. \quad (1)$$

The diffusion of radium-A radio-elements resulting from the disintegration of radon gas in air flowing through a cylindrical tube [1, 2], for instance, is depicted by such an equation. In this situation, v_x and v_r are, respectively, the axial and radial velocity components of the gas; c, the mass concentration of the radio-elements; D, their coefficient of diffusion; and q, the rate of formation of these radio-elements per unit volume of the following gas.

Since equation (1) is mathematically analogous to that of heat transfer in a cylindrical tube where q then denotes the rate of heat generation within the fluid, it is apparent that any solution of equation (1) is directly applicable to the corresponding heat transfer problem involving similar boundary conditions.

The usual assumptions made in the solution of equation (1) are those of negligible secondary flows and negligible diffusion in the axial direction, such that the terms involving v_r and $\partial^2 c/\partial x^2$ can be eliminated from the equation. Such a problem has been studied by Tan [1] in an earlier paper on diffusion involving a uniform-velocity, a parabolic-velocity, and a Langhaar-velocity profile.

The assumption of negligible secondary flows, i.e. $v_r = 0$, is probably justifiable for flows in relatively long tubes since its significance diminishes rapidly away from the tube inlet. In his analysis of heat transfer in the entrance region of cylindrical tubes, Kays [3] showed that the effect of the v_r term is quite small compared to the term on the left-hand side of equation (1) for $\xi > 0{\cdot}02$. The other assumption of negligible axial diffusion is not always justifiable, however, particularly for fluids with high diffusivities flowing at low mean velocities. Based on the simplifying assumption of a uniform-velocity profile, Schneider [4] has analyzed the effect of axial conduction on entrance-region heat transfer and concluded that it is quite appreciable if the Péclét number is <100. This conclusion is later confirmed by Hsu [5] in his exact mathematical analysis on entrance-region heat transfer for a Poiseuille pipe flow.

The need for neglecting axial diffusion in the traditional analysis is partly due to the fact that its inclusion in the diffusion equation will make the latter no longer amenable to known feasible mathematical manipulations. A basic mathematical difficulty arises since the differential equation then reduces to a Whittaker-type differential equation [4] for which the eigenfunctions are not orthogonal. This constitutes a major drawback in the computation of the coefficients of series expansion. To remedy this difficulty, Singh [6] expressed the eigenfunctions as an infinite series of Bessel functions of order zero which are orthogonal over the finite interval of integration. The differential equation for the problem is then reduced to an infinite set of linear simultaneous algebraic equations for the coefficients of the series. The technique, however, does not readily render higher eigenvalues, which are needed especially for small Péclét numbers. Hsu [5] has proposed a relatively simple mathematical scheme which, together with the aid of a high-speed digital computer, gives the pertinent eigenvalues and eigenfunctions. Moreover, this technique does not present any undue complication in determining the higher eigenvalues.

In this analysis of mass transfer with axial diffusion, a slug flow (uniform-velocity profile) and a Poiseuille pipe flow (parabolic-velocity profile) will be considered. For the latter case, the method used by Hsu [5] will be employed. Because of the Péclét number dependence, determination of the eigenvalues, eigenfunctions, and coefficients of series expansion will be given for $n = 1$–20 for arbitrarily selected Péclét numbers of 1, 5, 10, 20, 30, 50, 100 and ∞. In addition, asymptotic expressions for the eigenvalues for the corresponding Péclét numbers will be given.

MATHEMATICAL ANALYSIS

In brief, the diffusion problem of decaying products of an inert gas under consideration is to seek solution to equation (1) under the following boundary conditions:

$$c(0, r) = 0 \tag{2a}$$

$$c(\infty, r) = c_f \tag{2b}$$

$$\frac{\partial c}{\partial r}(x, 0) = 0 \tag{2c}$$

$$c(x, r_0) = 0. \tag{2d}$$

The first boundary condition is a constraint of an experimental technique reported in [2] of placing a high efficiency filter at the tube inlet to remove any particulate matter; the second is as a consequence of the requirement that, for large x, the solution should revert to the fully established concentration profile which has been given in [1] as

$$c_f = \frac{q r_0^2}{4D}\left(1 - \frac{r^2}{r_0^2}\right); \tag{3}$$

the third is the symmetry requirement at the center of the tube; and the last indicates complete annihilation of the radio-elements as they come in contact with the tube walls (see footnote on p. 473 of [1]).

To find the concentration solution satisfying equations (1) and (2), it is convenient to define a new concentration variable, $c^* = c - c_f$. Further, by introducing the following dimensionless parameters:

$$\psi = \frac{Dc}{q r_0^2}, \qquad \psi^* = \frac{Dc^*}{q r_0^2}$$

$$\Lambda_x = \frac{v_x}{V}, \qquad \Lambda_r = \frac{v_r}{V}$$

$$\eta = \frac{r}{r_0}, \qquad \xi = \frac{x}{r_0 Re \, . \, Sc}$$

where r_0 is the inner radius of the tube; V is the mean fluid velocity; and Re and Sc are, respectively, the Reynolds number and the Schmidt number; it can be readily shown that equations (1) and (2) become

$$\tfrac{1}{2}\Lambda_x \frac{\partial \psi^*}{\partial \xi} + \tfrac{1}{2} Pe \; \Lambda_r\left(\frac{\partial \psi^*}{\partial \eta} - \tfrac{1}{2}\eta\right) = \frac{1}{\eta}\frac{\partial}{\partial \eta}\left(\eta \frac{\partial \psi^*}{\partial \eta}\right) + \left(\frac{1}{Pe}\right)^2 \frac{\partial^2 \psi^*}{\partial \xi^2} \tag{4}$$

and

$$\psi^*(0, \eta) = -\tfrac{1}{4}(1 - \eta^2) \tag{5a}$$

$$\psi^*(\infty, \eta) = 0 \tag{5b}$$

$$\frac{\partial \psi^*}{\partial \eta}(\xi, 0) = 0 \tag{5c}$$

$$\psi^*(\xi, 1) = 0. \tag{5d}$$

The Péclét number of diffusion has been defined as $Pe = Re \cdot Sc$.

In this study, solutions are sought to satisfy equations (4) and (5) for a slug flow (uniform-velocity profile) and a Poiseuille pipe flow (parabolic-velocity profile). The required solutions will be expressed in the same form as that for the case of no axial diffusion. The latter may then be regarded as a special case of the more general problem in which axial diffusion is taken into account.

Solution for uniform-velocity profile

With the simplifying assumption of a uniform-velocity profile as in slug flow, i.e. $\Lambda_x = 1$ and $\Lambda_r = 0$, and letting $\mu = 2\xi$, equation (4) reduces to

$$\frac{\partial \psi^*}{\partial \mu} = \frac{1}{\eta}\frac{\partial}{\partial \eta}\left(\eta \frac{\partial \psi^*}{\partial \eta}\right) + \left(\frac{2}{Pe}\right)^2 \frac{\partial^2 \psi^*}{\partial \mu^2}. \tag{6}$$

Assuming the solution in the same form as that for the case of no axial diffusion [1]:

$$\psi^*(\mu, \eta) = \sum_{n=1}^{\infty} A_n P_n(\eta) \exp(-\lambda_n^2 \mu) \tag{7}$$

which automatically satisfies the boundary condition (5b), one finds that the eigenvalues λ_n and the eigenfunctions $P_n(\eta)$ must be solutions of the following ordinary differential equation:

$$P_n'' + \frac{1}{\eta} P_n' + \alpha_n^2 P_n = 0 \tag{8}$$

with

$$P_n'(0) = 0 \quad \text{and} \quad P_n(1) = 0 \tag{9}$$

where the prime designates derivative with respect to η and

$$\alpha_n^2 = \lambda_n^2 \left[1 + \left(\frac{2\lambda_n}{Pe}\right)^2\right]. \tag{10}$$

Furthermore, to fulfil the initial conditions of (5a), the coefficients of series expansion, A_n, in equation (7) must be determined such that

$$\sum_{n=1}^{\infty} A_n P_n(\eta) = -\tfrac{1}{4}(1 - \eta^2). \tag{11}$$

It can be readily shown from equations (8) and (9) that $P_n(\eta)$ are expressible in terms of the Bessel functions $J_0(\lambda_n \eta)$, and from equation (11) that

$$A_n = -\frac{2}{\alpha_n^3}\frac{1}{J_1(\alpha_n)}$$

where $\pm\alpha_n$, $n = 1, 2, 3, \ldots$ are the positive roots of $J_0(\alpha) = 0$.

The solution to equation (6), satisfying equation (5), is thus

$$\psi^*(\mu, \eta) = -\sum_{n=1}^{\infty}\left(\frac{2}{\alpha_n^3}\right)\frac{J_0(\alpha_n \eta)}{J_1(\alpha_n)} \exp(-\lambda_n^2 \mu) \tag{12}$$

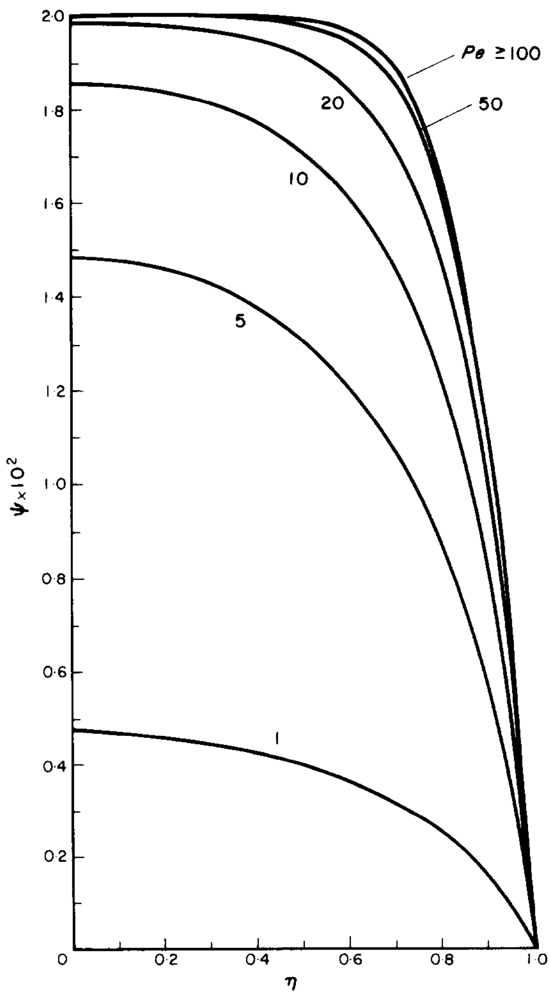

FIG. 1. Concentration profiles at $\xi = 0{\cdot}01$ for a slug flow.

Table 1. Eigenvalues and the related constants

(1) $Pe = 1$

n	λ_n	β_n	$[\beta_n]_{\text{asym.}}$	C_n	$R_n'(1)$	$[R_n'(1)]_{\text{asym.}}$	$\int_0^1 \eta R_n \, d\eta$
1	1·041101	1·429814	1·431780	−0·281627	−1·177306	−1·140826	0·210193
2	1·624152	2·277574	2·275163	0·040683	1·823589	1·817240	−0·065551
3	2·050285	2·885039	2·883344	−0·012850	−2·304607	−2·301927	0·032992
4	2·402518	3·385464	3·384265	0·005761	2·702752	2·701209	−0·020511
5	2·709521	3·821061	3·820166	−0·003131	−3·049794	−3·048765	0·014285
6	2·985196	4·211932	4·211234	0·001917	3·361381	3·360635	−0·010672
7	3·237523	4·569539	4·568976	−0·001272	−3·646533	−3·645964	0·008359
8	3·471581	4·901154	4·900687	0·000894	3·911001	3·910554	−0·006775
9	3·690841	5·211732	5·211335	−0·000656	−4·158711	−4·158360	0·005635
10	3·897796	5·504828	5·504485	0·000498	4·392488	4·392216	−0·004782
11	4·094310	5·783100	5·782798	−0·000389	−4·614439	−4·614245	0·004125
12	4·281819	6·048590	6·048320	0·000310	4·826187	4·826076	−0·003605
13	4·446145	6·302915	6·302668	−0·000253	−5·029009	−5·028998	0·003186
14	4·634140	6·547373	6·547144	0·000208	5·223934	5·224047	−0·002842
15	4·800618	6·783032	6·782816	−0·000175	−5·411799	−5·412076	0·002556
16	4·961514	7·010780	7·010570	0·000148	5·593298	5·593792	−0·002315
17	5·117355	7·231363	7·231155	−0·000127	−5·769010	−5·769792	0·002109
18	5·268590	7·445419	7·445208	0·000109	5·939421	5·940584	−0·001932
19	5·415603	7·653496	7·653277	−0·000096	−6·104940	−6·106605	0·001779
20	5·558731	7·856070	7·855838	0·000 083	6·265915	6·268236	−0·001644

(2) $Pe = 5$

n	λ_n	β_n	$[\beta_n]_{\text{asym.}}$	C_n	$R_n'(1)$	$[R_n'(1)]_{\text{asym.}}$	$\int_0^1 \eta R_n \, d\eta$
1	1·910689	2·385304	2·501045	−0·287856	−1·061607	−0·851135	0·200744
2	3·320330	4·510940	4·531754	0·049995	1·649596	1·609615	−0·074750
3	4·328262	5·976526	5·981138	−0·017237	−2·143837	−2·132572	0·038662
4	5·149661	7·157913	7·158903	0·007656	2·558767	2·554120	−0·023639
5	5·859426	8·174395	8·174344	−0·004019	−2·919289	−2·916826	0·016127
6	6·493120	9·079841	9·079455	0·002376	3·241436	3·239912	−0·011841
7	7·070791	9·903999	9·903509	−0·001531	−3·535032	−3·533992	0·009149
8	7·605020	10·66535	10·664844	0·001052	3·806416	3·805661	−0·007336
9	8·104301	11·37631	11·375817	−0·000758	−4·059914	−4·059349	0·006050
10	8·574686	12·04568	12·045211	0·000567	4·298622	4·298197	−0·005098
11	9·020663	12·67998	12·679531	−0·000437	−4·524838	−4·524531	0·004372
12	9·445668	13·28417	13·283751	0·000345	4·740318	4·740121	−0·003803
13	9·852401	13·86218	13·861773	−0·000278	−4·946445	−4·946369	0·003347
14	10·24303	14·41711	14·416724	0·000228	5·144320	5·144382	−0·002975
15	10·61932	14·95154	14·951157	−0·000190	−5·334842	−5·335080	0·002668
16	10·98275	15·46757	15·467187	0·000159	5·518748	5·519212	−0·002409
17	11·33455	15·96698	15·966589	−0·000137	−5·696655	−5·697414	0·002190
18	11·67577	16·45128	16·450871	0·000116	5·869077	5·870224	−0·002002
19	12·00731	16·92176	16·921326	−0·000102	−6·036449	−6·038103	0·001840
20	12·32994	17·37955	17·379074	0·000088	6·199139	6·201454	−0·001698

Table 1—continued

(3) $Pe = 100$

n	λ_n	β_n	$[\beta_n]_{\text{asym.}}$	C_n	$R_n'(1)$	$[R_n'(1)]_{\text{asym.}}$	$\int_0^1 \eta R_n \, d\eta$
1	2·201009	2·596931	2·805146	−0·288188	−1·030610	−0·655239	0·198164
2	4·218890	5·546884	5·622804	0·051765	1·521785	1·399552	−0·079184
3	5·704213	7·713849	7·739680	−0·019739	−1·985494	−1·946305	0·043569
4	6·911455	9·459211	9·469257	0·009348	2·401592	2·386683	−0·027088
5	7·949455	10·95320	10·957957	−0·005003	−2·770527	−2·763636	0·018380
6	8·872196	12·27805	12·280100	0·002942	3·101652	3·097914	−0·013335
7	9·710421	13·47957	13·480528	−0·001867	−3·403357	−3·401073	0·010177
8	10·48343	14·58622	14·586628	0·001260	3·681813	3·680295	−0·008071
9	11·20422	15·61707	15·617177	−0·000893	−3·941458	−3·940392	0·006594
10	11·88201	16·58561	16·585553	0·000658	4·185536	4·184768	−0·005513
11	12·52362	17·50176	17·501590	−0·000501	−4·416480	−4·415925	0·004696
12	13·13424	18·37312	18·372882	0·000391	4·636159	4·635780	−0·004061
13	13·71794	19·20560	19·205317	−0·000312	−4·846040	−4·845826	0·003557
14	14·27797	20·00393	20·003617	0·000254	5·047297	5·047255	−0·003149
15	14·81698	20·77197	20·771627	−0·000210	−5·240884	−5·241042	0·002813
16	15·33716	21·51290	21·512525	0·000175	5·427586	5·427988	−0·002532
17	15·84036	22·22939	22·228973	−0·000149	−5·608055	−5·608768	0·002295
18	16·32812	22·92369	22·923227	0·000126	5·782835	5·783949	−0·002093
19	16·80179	23·59773	23·597217	−0·000110	−5·952389	−5·954018	0·001919
20	17·26250	24·25319	24·252610	0·000095	6·117103	6·119399	−0·001767

(4) $Pe = 10$

n	λ_n	β_n	$[\beta_n]_{\text{asym.}}$	C_n	$R_n'(1)$	$[R_n'(1)]_{\text{asym.}}$	$\int_0^1 \eta R_n \, d\eta$
1	2·402055	2·703129	2·997341	−0·286540	−1·014490	−0·215678	0·196814
2	5·487135	6·65757	6·967179	0·049769	1·352788	0·531197	−0·082914
3	8·530468	10·58267	10·877234	−0·019945	−1·587621	−0·844374	0·052314
4	11·49190	14·43472	14·701964	0·010782	1·786051	1·151723	−0·037951
5	14·35144	18·18979	18·423251	−0·006804	−1·971889	−1·451335	0·029484
6	17·09886	21·83222	22·029869	0·004712	2·156333	1·741958	−0·023810
7	19·73091	25·35315	25·516311	−0·003465	−2·344676	−2·022888	0·019687
8	22·24912	28·74932	28·881434	0·002650	2·538816	2·293863	−0·016525
9	24·65801	32·02164	32·127179	−0·002083	−2·738571	−2·554957	0·014013
10	26·96373	35·17390	35·257511	0·001665	2·942621	2·806470	−0·011971
11	29·17319	38·21163	38·277614	−0·001349	−3·149157	−3·048846	0·010287
12	31·29342	41·14123	41·193308	0·001100	3·356319	3·282594	−0·008886
13	33·33126	43·96944	44·010644	−0·000905	−3·562490	−3·508253	0·007715
14	35·29316	46·70290	46·735647	0·000747	3·766375	3·727149	−0·006733
15	37·18507	49·34799	49·374148	−0·000621	−3·967045	−3·937399	0·005906
16	39·01244	51·91070	51·931691	0·000516	4·163881	4·141874	−0·005208
17	40·78023	54·39659	54·413483	−0·000434	−4·356514	−4·340219	0·004618
18	42·49291	56·81076	56·824372	0·000362	4·544751	4·532842	−0·004116
19	44·15453	59·15793	59·168854	−0·000309	−4·728537	−4·720119	0·003688
20	45·76873	61·44239	61·451077	0·000259	4·907891	4·902393	−0·003321

Table 1—continued

(5) $Pe = \infty$ (No axial diffusion)

n	λ_n	β_n	C_n	$R_n'(1)$	$\int_0^1 \eta R_n \, d\eta$
1	2.404825	2.704364	−0.286463	−1.014300	0.196798
2	5.520078	6.679031	0.049572	1.349241	−0.082971
3	8.653727	10.67338	−0.019679	−1.572319	0.052554
4	11.791534	14.67108	0.010483	1.746004	−0.038465
5	14.930917	18.66987	−0.006498	−1.890852	0.030337
6	18.071063	22.66915	0.004419	2.016461	−0.025047
7	21.211636	26.66868	−0.003199	−2.128157	0.021330
8	24.352471	30.66835	0.002422	2.229232	−0.018574
9	27.493479	34.66813	−0.001898	−2.321909	0.016449
10	30.634606	38.66798	0.001526	2.407722	−0.014761
11	33.775820	42.66789	−0.001255	−2.487811	0.013387
12	36.917098	46.66786	0.001049	2.563038	−0.012247
13	40.058425	50.66788	−0.000892	−2.634056	0.011286
14	43.199791	54.66797	0.000764	2.701408	−0.010465
15	46.341188	58.66814	−0.000666	−2.765517	0.009755
16	49.482609	62.66839	0.000581	2.826715	−0.009135
17	52.624051	66.66873	−0.000517	−2.885277	0.008589
18	55.765510	70.66920	0.000456	2.941461	−0.008104
19	58.906983	74.66979	−0.000414	−2.995421	0.007671
20	62.048469	78.67054	0.000367	3.047334	−0.007281

and the complete concentration solution is

$$\psi(\mu, \eta) = \tfrac{1}{4}(1 - \eta^2) - \sum_{n=1}^{\infty}\left(\frac{2}{\alpha_n^3}\right) \times \frac{J_0(\alpha_n \eta)}{J_1(\alpha_n)} \exp(-\lambda_n^2 \mu) \tag{13}$$

where λ_n is related to α_n, the roots of $J_0(\alpha_n) = 0$, through equation (10). It should be pointed out that equation (13) differs from that of the case of no axial diffusion only in that λ_n are now the eigenvalues which are dependent on the Péclét number. As the Péclét number approaches infinity, however, $\lambda_n \to \alpha_n$ and equation (13) reverts to the corresponding equation for the case of no axial diffusion [1].

The first twenty eigenvalues, λ_n, are tabulated in Table 1 for Péclét numbers of 1, 5, 10, 100 and ∞. It is noted that at small Péclét numbers the consecutive higher eigenvalues do not vary appreciably in magnitude. This means that in the series summation, as in equation (13), the series converges slowly at smaller Péclét numbers, necessitating an increase in the number of eigenvalues to be included in the computation. The concentration profiles calculated from equation (13) at $\xi = 0.01$ ($\mu = 0.02$) are shown

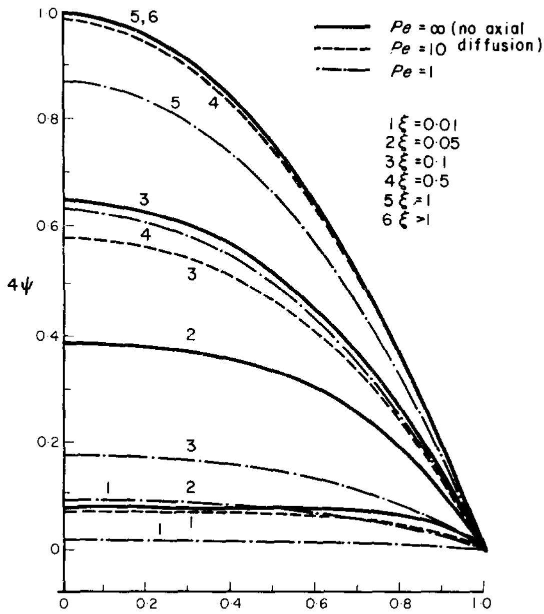

FIG. 2. Variation of entrance-region concentration profiles for a slug flow.

in Fig. 1 for several Péclét numbers. It is seen that the effect of axial diffusion is a greater decrease in the mass concentration, the smaller the Péclét number. Variations of the entrance-region concentration profiles are illustrated in Fig. 2 for $Pe = 1$, 10 and ∞. It is observed that for $Pe > 1$, the concentration profiles at $\xi \geqslant 1$ already approach the fully established profile given by equation (3).

Solution for parabolic-velocity profile

For the Poiseuille pipe flow, $\Lambda_x = 2(1-\eta^2)$ and $\Lambda_r = 0$ and equation (4) becomes

$$(1-\eta^2)\frac{\partial\psi^*}{\partial\xi} = \frac{1}{\eta}\frac{\partial}{\partial\eta}\left(\eta\frac{\partial\psi^*}{\partial\eta}\right) + \left(\frac{1}{Pe}\right)^2\frac{\partial^2\psi^*}{\partial\xi^2} \quad (14)$$

to be satisfied by the same boundary conditions depicted by equation (5). Again, one seeks solution in the same form as that for the case of no axial diffusion, i.e.

$$\psi^*(\xi,\eta) = \sum_{n=1}^{\infty} C_n R_n(\eta)\exp(-\beta_n^2\xi). \quad (15)$$

Substitution of the above into equations (5) and (14) yields

$$R_n'' + \frac{1}{\eta}R_n' + \beta_n^2 \times \left[(1-\eta^2) + \left(\frac{\beta_n}{Pe}\right)^2\right]R_n = 0 \quad (16)$$

with

$$R_n'(0) = 0 \quad \text{and} \quad R_n(1) = 0 \quad (17)$$

and the following relationship

$$\sum_{n=1}^{\infty} C_n R_n(\eta) = -\tfrac{1}{4}(1-\eta^2) \quad (18)$$

necessary for the determination of the coefficients of series expansion, C_n.

Because Singh's method [6] does not readily render higher eigenvalues which are needed especially for small Péclét numbers, Hsu's method is employed here. Following Hsu [5], the eigenvalues, β_n, and eigenfunctions, $R_n(\eta)$, are determined directly by solving equation (16) with the aid of a CDC-6600 computer using the Runge–Kutta scheme. For each preassigned value of Péclét number, the eigenvalues are determined by trial and error procedure so that equations (16) and (17) are simultaneously satisfied. The first twenty values of β_n thus determined are tabulated in Table 1 for Péclét number of 1, 5, 10, 100 and ∞. The eigenvalues are seen to increase with increasing Péclét numbers and approach asymptotically those for the case of no axial diffusion. It is again noted that at small Péclét numbers the consecutive higher eigenvalues do not vary appreciably in magnitude. The quantity $R_n'(1)$ is related to the mass flux at the wall and occurs frequently in subsequent analyses and is thus included in Table 1.

It is noted that the eigenfunctions, $R_n(\eta)$, are not mutually orthogonal and, as such, the eigenfunction expansion technique widely used for the "Sturm–Liouville" system cannot be utilized here in evaluating the coefficients C_n. However, multiplying both sides of equation (18) by $\eta R_n[g(\eta,\beta) - g(\eta,\beta_n)]$, integrating from 0 to 1, and utilizing l'Hospital's rule, the series coefficients, C_n, can be found to be

$$C_n = \frac{-\dfrac{1}{4}\displaystyle\int_0^1 \eta(1-\eta^2)R_n\left(\frac{\partial g}{\partial\beta}\right)_{\beta=\beta_n}\mathrm{d}\eta - \sum_{\substack{m=1\\ m\neq n}}^{\infty} C_m\int_0^1 \eta R_m R_n\left(\frac{\partial g}{\partial\beta}\right)_{\beta=\beta_n}\mathrm{d}\eta}{\displaystyle\int_0^1 \eta R_n^2\left(\frac{\partial g}{\partial\beta}\right)_{\beta=\beta_n}\mathrm{d}\eta}$$

$$= \frac{-\frac{1}{4}\int_0^1\left[(1-\eta^2)+2\left(\frac{\beta_n}{Pe}\right)^2\right]\eta(1-\eta^2)R_n\,d\eta-\sum_{\substack{m=1\\m\neq n}}^{\infty}C_m\int_0^1\left[(1-\eta^2)+2\left(\frac{\beta_n}{Pe}\right)^2\right]\eta R_m R_n\,d\eta}{\int_0^1\left[(1-\eta^2)+2\left(\frac{\beta_n}{Pe}\right)^2\right]\eta R_n^2\,d\eta} \tag{19}$$

where $g(\eta, \beta_n) = \beta_n^2\,[(1-\eta^2)+(\beta_n/Pe)^2]$ and β is considered as a parameter. Utilizing the relationship

$$\int_0^1\left[(1-\eta^2)+\frac{\beta_n^2+\beta_m^2}{(Pe)^2}\right]\eta R_m R_n\,d\eta = 0 \qquad (m \neq n) \tag{20}$$

obtainable from equation (16), the infinite series in equation (19) can be simplified, and thus

$$C_n = \frac{-\frac{1}{4}\int_0^1\left[(1-\eta^2)+2\left(\frac{\beta_n}{Pe}\right)^2\right]\eta(1-\eta^2)R_n\,d\eta-\frac{1}{(Pe)^2}\sum_{\substack{m=1\\m\neq n}}^{\infty}(\beta_n^2-\beta_m^2)\,C_m\int_0^1\eta R_m R_n\,d\eta}{\int_0^1\left[(1-\eta^2)+2\left(\frac{\beta_n}{Pe}\right)^2\right]\eta R_n^2\,d\eta}. \tag{21}$$

Let

$$-\frac{1}{4}\int_0^1\left[(1-\eta^2)+2\left(\frac{\beta_n}{Pe}\right)^2\right] \times \eta(1-\eta^2)R_n\,d\eta = I_n$$

$$\int_0^1\left[(1-\eta^2)+2\left(\frac{\beta_n}{Pe}\right)^2\right]\eta R_n^2\,d\eta = J_n$$

$$\frac{1}{(Pe)^2}(\beta_n^2-\beta_m^2)\int_0^1\eta R_m R_n\,d\eta = \Gamma_{n,m}$$

equation (21) can be written as

$$C_n J_n + \sum_{\substack{m=1\\m\neq n}}^{\infty}\Gamma_{n,m}C_m = I_n \quad (n = 1, 2, 3, \ldots). \tag{22}$$

Equation (22) represents a set of infinite simultaneous equations which can then be solved for the unknowns, C_n. In this study, the infinite series was truncated at $m = 20$, which was found to give satisfactory converging solutions. It was further shown that by choosing $m > 20$ it does not significantly improve the solutions. With $m = 20$, equation (22) gives rise to 20 simultaneous equations which were solved by utilizing the "Gauss elimination technique" with a CDC-6600 computer. Thus, let

$$\{A\} = \begin{bmatrix} J_1 & \Gamma_{1,2} & \Gamma_{1,3} & \cdots\Gamma_{1,20} \\ \Gamma_{2,1} & J_2 & \Gamma_{2,3} & \cdots\Gamma_{2,20} \\ \cdot & & & \cdot \\ \cdot & & & \cdot \\ \cdot & & & \cdot \\ \Gamma_{20,1} & \Gamma_{20,2} & \Gamma_{20,3} & \cdots J_{20} \end{bmatrix}$$

$$\{X\} = \begin{bmatrix} C_1 \\ C_2 \\ C_3 \\ \cdot \\ \cdot \\ \cdot \\ C_{20} \end{bmatrix}, \quad \{B\} = \begin{bmatrix} I_1 \\ I_2 \\ I_3 \\ \cdot \\ \cdot \\ \cdot \\ I_{20} \end{bmatrix}$$

equation (22) can be written in a matrix form as

$$\{X\} = \{A\}^{-1}\{B\} \tag{23}$$

where $\{A\}^{-1}$ is the inverse of matrix $\{A\}$. The coefficients of series expansion, C_n, are determined from equation (23) and tabulated in Table 1. The calculated C_n coefficients were actually substituted into equation (18) and it was ascertained that they indeed satisfy equation (18) very well. This can, in fact, be regarded as a proof of the mathematical correctness of the present solutions.

It is noted that the diagonal elements of the matrix, $\{A\}$, are actually dominating. In other words, the off-diagonal elements, $\Gamma_{n,m}$, are, in general, much smaller than J_n. In fact, as $Pe \to \infty$, $\Gamma_{n,m} \to 0$. This indicates that the terms in the infinite series in equation (21) are small and may be neglected. Approximately, therefore, one can calculate C_n from the following equation directly without solving a set of simultaneous equations.

$$C_n = \frac{-\frac{1}{4}\int_0^1 [(1-\eta^2) + 2(\beta_n/Pe)^2] \times \eta(1-\eta^2) R_n \, d\eta}{\int_0^1 [(1-\eta^2) + 2(\beta_n/Pe)^2] \, \eta \, R_n^2 \, d\eta}. \tag{24}$$

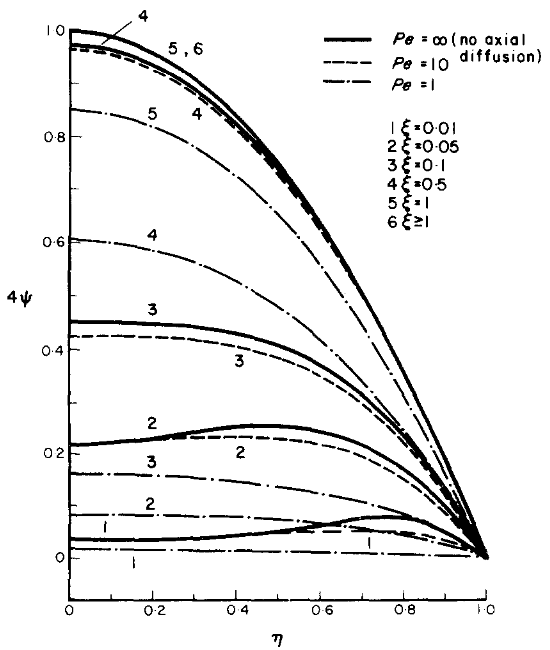

FIG. 3. Variation of entrance-region concentration profiles for a Poiseuille pipe flow.

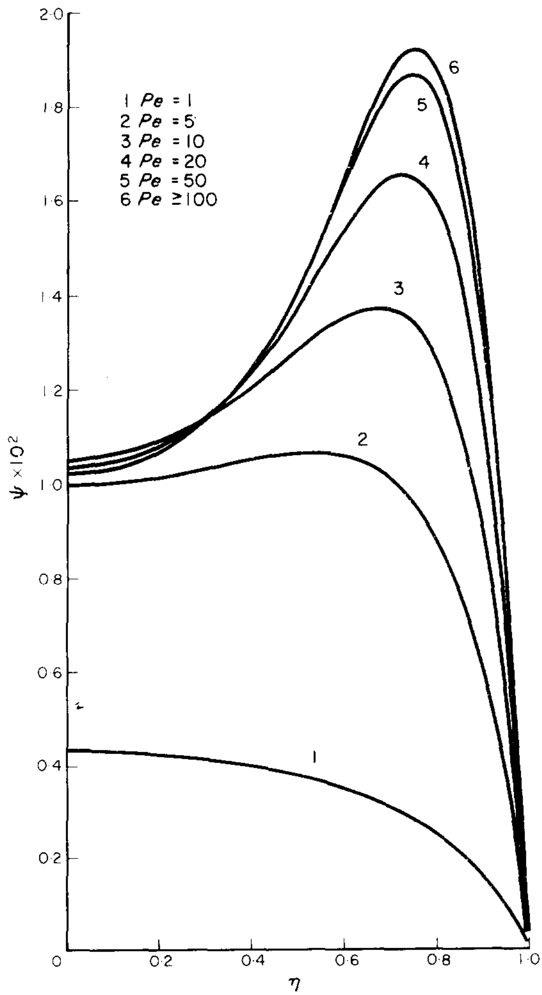

FIG. 4. Concentration profiles at $\xi = 0{\cdot}01$ for a Poiseuille pipe flow.

Errors introduced by such an approximation are small ($\simeq$ 2–3 per cent).

The complete concentration solution, thus, is given by

$$\psi(\xi, \eta) = \tfrac{1}{4}(1 - \eta^2) + \sum_{n=1}^{\infty} C_n R_n(\eta) \exp(-\beta_n^2 \xi). \quad (25)$$

Some typical profiles are shown in Fig. 3 for Pe = 1, 10 and ∞. It is observed that again in this case of Poiseuille pipe flow, the concentration profiles at $\xi \geqslant 1$ for $Pe > 1$ almost coincide with that representing the case of no axial diffusion. The concentration profiles at $\xi = 0{\cdot}01$ are shown in Fig. 4 for several Péclét numbers. It is interesting to observe that, in comparison with the corresponding profiles based on the slug flow (Fig. 2), the concentrations are greatly reduced in the central core, apparently due to the accelerated central-core flow in the Poiseuille pipe flow.

The trial and error procedure used in determining the eigenvalues β_n from equations (16) and (17) can be facilitated by finding the asymptotic expression for the eigenvalues. Following Sellars *et al.* [7] and taking into consideration the effect of axial diffusion, the eigenfunctions $R_n(\eta)$, for $0 < \eta \leqslant 1$ and sufficiently large β_n, may be given by the so-called WKB approximations:

$$R_n(\eta) = \frac{\cos\{\beta_n \int_0^{\eta} [1 - \zeta^2 + (\beta_n/Pe)^2]^{\frac{1}{2}} \, d\zeta - \pi/4\}}{(\pi\beta_n\eta/2)^{\frac{1}{2}} [1 - \eta^2 + (\beta_n/Pe)^2]^{\frac{1}{4}}}$$

$$= \frac{\cos\{(\beta_n/2)\,\eta\sqrt{[1 - \eta^2 + (\beta_n/Pe)^2]} + (\beta_n/2)[1 + (\beta_n/Pe)^2] \sin^{-1}(\eta/\sqrt{[1 + (\beta_n/Pe)^2]}) - \pi/4\}}{(\pi\beta_n\eta/2)^{\frac{1}{2}} [1 - \eta^2 + (\beta_n/Pe)^2]^{\frac{1}{4}}}. \quad (26)$$

To satisfy the boundary condition $R_n(1) = 0$, it is required that

$$\left(\frac{\beta_n}{2}\right)\left\{\left(\frac{\beta_n}{Pe}\right) + \left[1 + \left(\frac{\beta_n}{Pe}\right)^2\right] \times \sin^{-1}\left[\frac{1}{\sqrt{[1 + (\beta_n/Pe)^2]}}\right]\right\} = \pi(n - \tfrac{1}{4}). \quad (27)$$

The roots of equation (27) for an arbitrarily preassigned value of Péclét number represent, therefore, the desired asymptotic eigenvalues for the particular Péclét number. These values are included in Table 1 for comparison with the exact values obtained by directly solving equations (16) and (17). It is surprising to note that whereas the asymptotic expression is supposed to be valid for very large β, in actuality values of n as small as 1 for Pe = 1, 2 for Pe = 5, 3 for Pe = 10, 4 for Pe = 20, 5 for Pe = 30, 6 for Pe = 50, and 8 for Pe = 100 give errors of β only within 0·5 per cent of the actual values.

From equation (26), the asymptotic expression for the first derivative of the eigenfunction at the wall can be found to be

$$R_n'(1) = (-1)^n \sqrt{\left(\frac{2}{\pi}\right)} \frac{\beta_n}{\sqrt{Pe}} \qquad = 1, 2, \ldots). \quad (28)$$

The asymptotic values of $R_n'(1)$, denoted by $[R_n'(1)]_{\text{asym.}}$, are also tabulated in Table 1 for comparison with the actual values.

PHYSICAL ANALYSES

The aforementioned mathematical analyses give the local concentration distributions of the radio-elements within the cylindrical tube and, thus, provide the basis for such physical analyses as the local bulk concentration, the local Sherwood number, and the parameter $F_f(\xi)$ used in the experimental determination of the coefficient of diffusion [1, 2].

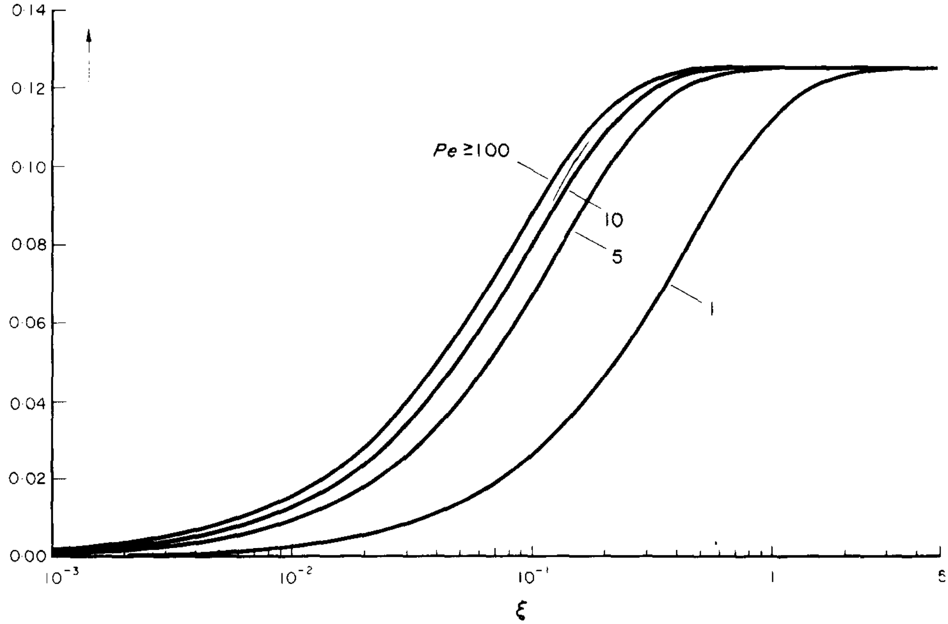

FIG. 5. Variation of bulk concentration in the entrance-region of a slug flow.

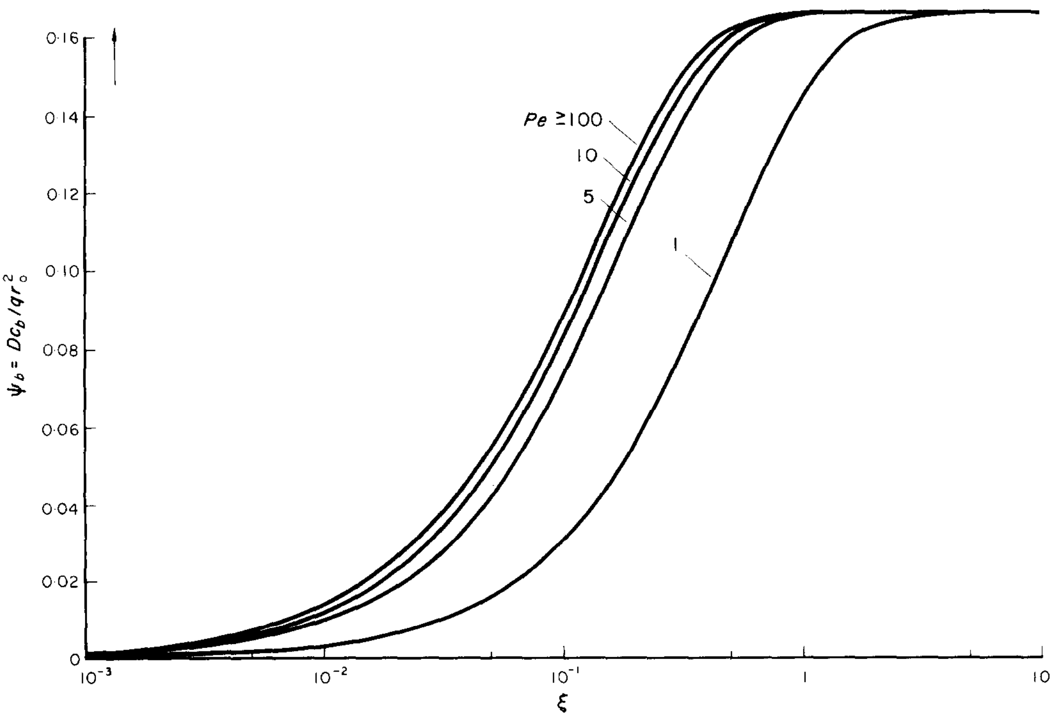

FIG. 6. Variation of bulk concentration in the entrance-region of a Poiseuille pipe flow.

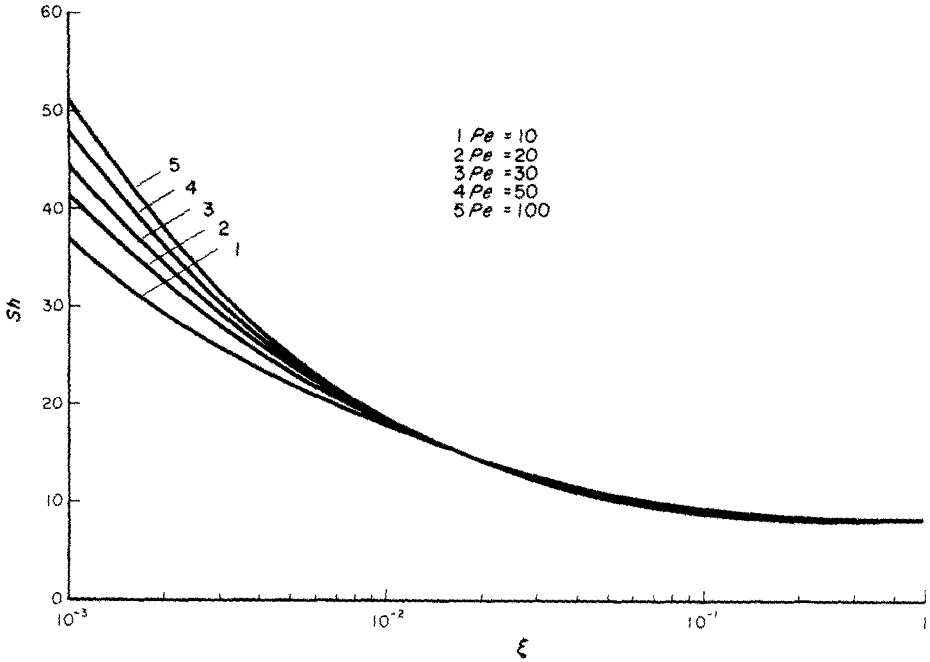

FIG. 7. Variations of Sherwood number in the entrance-region of a slug flow.

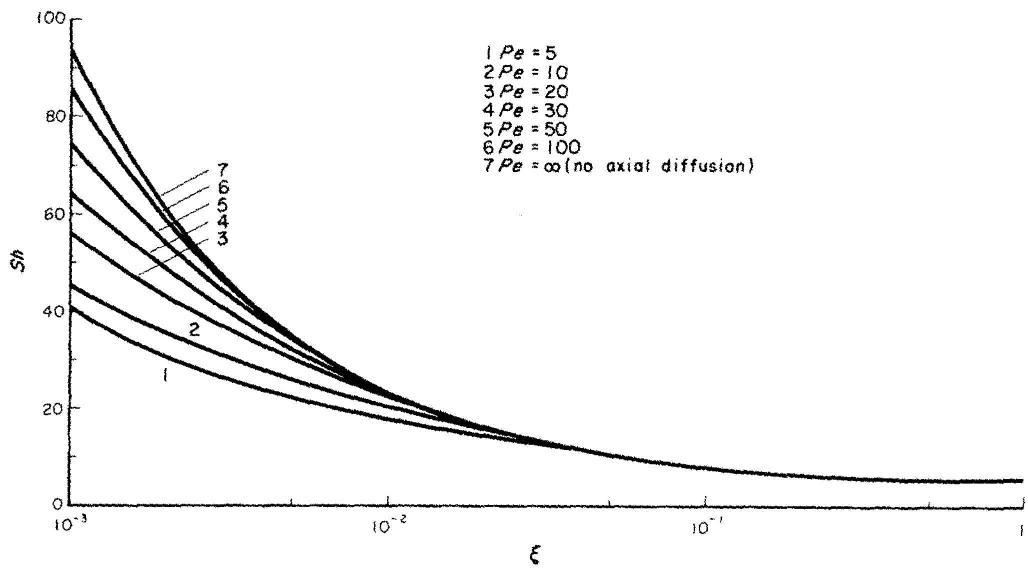

FIG. 8. Variations of Sherwood number in the entrance-region of a Poiseuille pipe flow.

Local bulk concentration and Sherwood number

Defining the local bulk concentration as

$$c_b = \frac{\int_0^{r_0} v_x c r \, \mathrm{d}r}{\int_0^{r_0} v_x r \, \mathrm{d}r}$$

we get,

$$\psi_b(\xi) = \frac{Dc_b}{qr_0^2} = \frac{\int_0^1 \Lambda_x(\xi,\eta)\,\psi(\xi,\eta)\,\eta\,\mathrm{d}\eta}{\int_0^1 \Lambda_x(\xi,\eta)\,\eta\,\mathrm{d}\eta}. \quad (29)$$

It can be readily shown that for the uniform-velocity flow,

$$\psi_b(\xi) = \sum_{n=1}^{\infty} \frac{4}{\alpha_n^4}[1 - \exp(-\lambda_n^2 \mu)] \quad (30a)$$

and that for the parabolic-velocity flow,

$$\psi_b(\xi) = \tfrac{1}{6} - 4\sum_{n=1}^{\infty} C_n\left[\left(\frac{1}{\beta_n}\right)^2 R_n'(1) + \left(\frac{\beta_n}{Pe}\right)^2 \int_0^1 \eta R_n \,\mathrm{d}\eta\right] \exp(-\beta_n^2 \xi). \quad (30b)$$

The first twenty values of $\int_0^1 \eta R_n \,\mathrm{d}\eta$ are also tabulated in Table 1 for the Péclét numbers considered herein. The bulk concentrations depicted by equations (30a) and (30b) are shown, respectively, in Figs. 5 and 6. As expected the local bulk concentration decreases with decreasing Péclét numbers. It is again observed that in both cases the fully established bulk concentration is approached at $\xi \geqslant 1$ for $Pe > 1$.

By the Ficks' law of diffusion, the mass flux density, I, at the wall is

$$I = -D\left[\frac{\partial c}{\partial r}\right]_{r=r_0} = -qr_0\left[\frac{\partial \psi}{\partial \eta}\right]_{\eta=1}.$$

Defining a mass-transfer coefficient, h_D, such that $h_D = I/c_b$, and invoking the above expression for the mass flux density, one obtains the local Sherwood number as

$$Sh = \frac{h_D(2r_0)}{D} = -\left(\frac{2}{\psi_b}\right)\left[\frac{\partial \psi}{\partial \eta}\right]_{\eta=1} \quad (31)$$

which, for the uniform-velocity flow,

$$Sh = 8\left\{\frac{1 - \sum_{n=1}^{\infty}(4/\alpha_n^2)\exp(-\lambda_n^2\mu)}{1 - \sum_{n=1}^{\infty}(32/\alpha_n^4)\exp(-\lambda_n^2\mu)}\right\} \quad (32a)$$

and, for the parabolic-velocity flow, is

$$Sh = 6\left\{\frac{1 - 2\sum_{n=1}^{\infty} C_n R_n'(1)\exp(-\beta_n^2\xi)}{1 - 24\sum_{n=1}^{\infty} C_n\left[(1/\beta_n)^2 R_n'(1) + (\beta_n/Pe)^2 \int_0^1 \eta R_n\,\mathrm{d}\eta\right]\exp(-\beta_n^2\xi)}\right\}. \quad (32b)$$

The local Sherwood numbers for both the uniform-velocity and parabolic-velocity profiles are, respectively, shown in Figs. 7 and 8 for various Péclét numbers. It is seen that in both cases the Sherwood number increases with increasing Péclét numbers at small ξ values; namely, $\xi < 0{\cdot}02$ for the uniform-velocity flow, and $\xi < 0{\cdot}04$ for the parabolic-velocity flow. At larger ξ values, however, the Sherwood number for a smaller Péclét number is slightly higher than that for a larger Péclét number. As $\xi \to \infty$, $Sh \to 8$ for the slug flow and $Sh \to 6$ for the Poiseuille pipe flow, independent of the Péclét numbers.

The parameters $F_f(\xi)$ *and* $F_f^*(\xi)$

The parameter $F_f(\xi)$, defined as the rate of the total particle flux over a cross-section at distance x from the tube inlet to the rate of formation of the radio-elements in the same volume element of the tube, i.e.

$$F_f(\xi) = \frac{2\pi \int_0^{r_0} v_x c r \, \mathrm{d}r}{\pi r_0^2 x q} = \frac{1}{\xi}\int_0^1 \Lambda_x(\xi, \eta)\, \psi(\xi, \eta)\, \eta \, \mathrm{d}\eta \qquad (33)$$

has been of great interest to experimenters in their laboratory determination of the coefficients of diffusion of disintegration products of an inert gas. The determination of the coefficient of diffusion of radium-A particles resulting from the disintegration of radon in air, carried out by Thomas *et al.* [2], is one such example.

The parameter $F_f(\xi)$ can be found for the uniform-velocity flow as:

$$F_f(\xi) = \frac{1}{\xi}\sum_{n=1}^{\infty}\left(\frac{2}{\alpha_n^4}\right)[1 - \exp(-\lambda_n^2 \mu)] \qquad (34a)$$

and for the parabolic-velocity flow as:

$$F_f(\xi) = \frac{1}{\xi}\left\{\frac{1}{12} - 2\sum_{n=1}^{\infty} C_n\left[\left(\frac{1}{\beta_n}\right)^2 R_n'(1) + \left(\frac{\beta_n}{Pe}\right)^2 \int_0^1 \eta R_n \, \mathrm{d}\eta\right]\exp(-\beta_n^2 \xi)\right\}. \qquad (34b)$$

The $F_f(\xi)$ values calculated from equations (34a) and (34b) are shown, respectively, in Figs. 9 and 10 for various Péclét numbers. It is seen that $F_f(\xi)$ values decrease with decreasing Péclét numbers. It is further observed that, in both the slug and Poiseuille pipe flows, the curve for $Pe = 100$ deviates from that for $Pe = \infty$ at $\xi < 0{\cdot}02$, more at smaller ξ values. This indicates that for $Pe \leqslant 100$, the effect of axial diffusion is still significant for $\xi < 0{\cdot}02$. In fact· from Figs. 9 and 10, it is observed that the effect of axial diffusion is negligible only for $Pe = 100$ and $\xi > 0{\cdot}02$; $Pe = 50$ and $\xi > 0{\cdot}1$; $Pe = 10$ and $\xi > 0{\cdot}5$; and $Pe = 1$ and $\xi > 5$ (not shown). Recalling that $\xi = x/(r_0 \,.\, Pe)$, it can thus be concluded that the effect of axial diffusion may be neglected at an axial distance from the tube inlet greater than two and a half times that of the tube diameter for $1 < Pe < 100$.

In defining the parameter $F_f(\xi)$, the local axial particle flux has been taken to be the convective flux given by the product of the local concentration and local fluid velocity, i.e. $f_x = v_x c$. To account for axial diffusive flux in the presence of axial diffusion, the axial particle flux should become $f_x = v_x c - D(\partial c/\partial x)$. One can thus define a new parameter $F_f^*(\xi)$ as

$$F_f^*(\xi) = \frac{2\pi \int_0^{r} [v_x c - D(\partial c/\partial x)] r \, \mathrm{d}r}{\pi r_0^2 x q} = \frac{1}{\xi}\int_0^1 \left[\Lambda_x \psi - \frac{2}{(Pe)^2}\frac{\partial \psi}{\partial \xi}\right]\eta \, \mathrm{d}\eta \qquad (35)$$

which reverts to $F_f(\xi)$ as $Pe \to \infty$. With this redefinition, one obtains

$$F_f^*(\xi) = \frac{1}{\xi}\left\{\frac{1}{16} - 2\sum_{n=1}^{\infty}\frac{1}{\lambda_n^4[1 + (2\lambda_n/Pe)^2]} \times \exp(-\lambda_n^2 \mu)\right\} \qquad (36a)$$

for the uniform-velocity flow, and

$$F_f^*(\xi) = \frac{1}{\xi}\left\{\frac{1}{12} - 2\sum_{n=1}^{\infty}\frac{C_n}{\beta_n^2}R_n'(1) \times \exp(-\beta_n^2 \xi)\right\} \qquad (36b)$$

for the parabolic-velocity flow.

The $F_f^*(\xi)$ values calculated from equations (36a) and (36b) are, respectively, shown in Fig. 11 and 12. Because the particle flux due to axial diffusion is in the negative x-direction in the entrance-region for finite values of Péclét numbers (see Figs. 2 and 3), the $F_f^*(\xi)$ values decrease markedly with decreasing Péclét numbers. At small ξ values, $F_f^*(\xi)$ values become

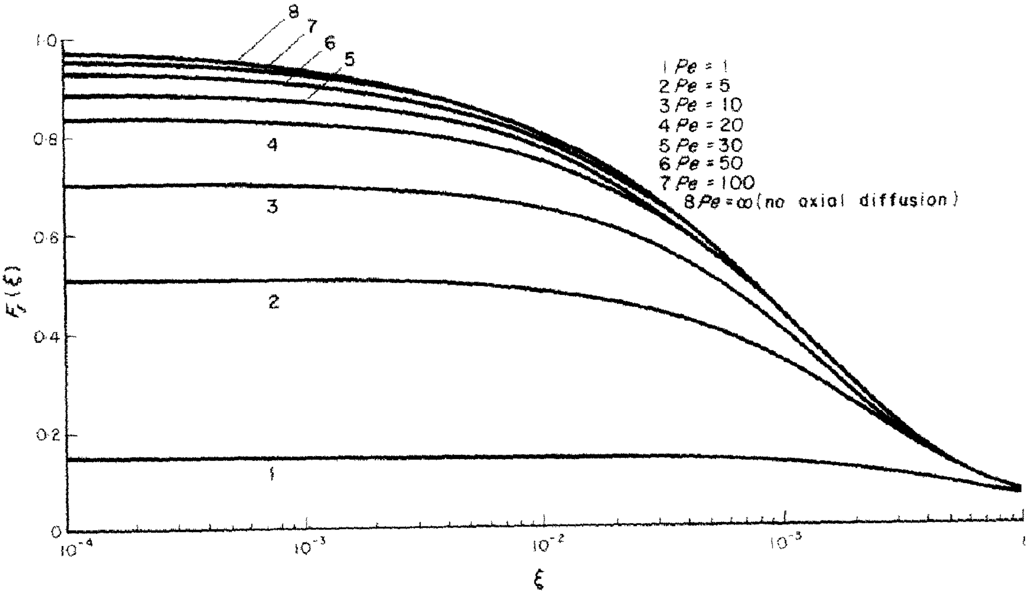

FIG. 9. Variation of $F_f(\xi)$ in the entrance-region of a slug flow.

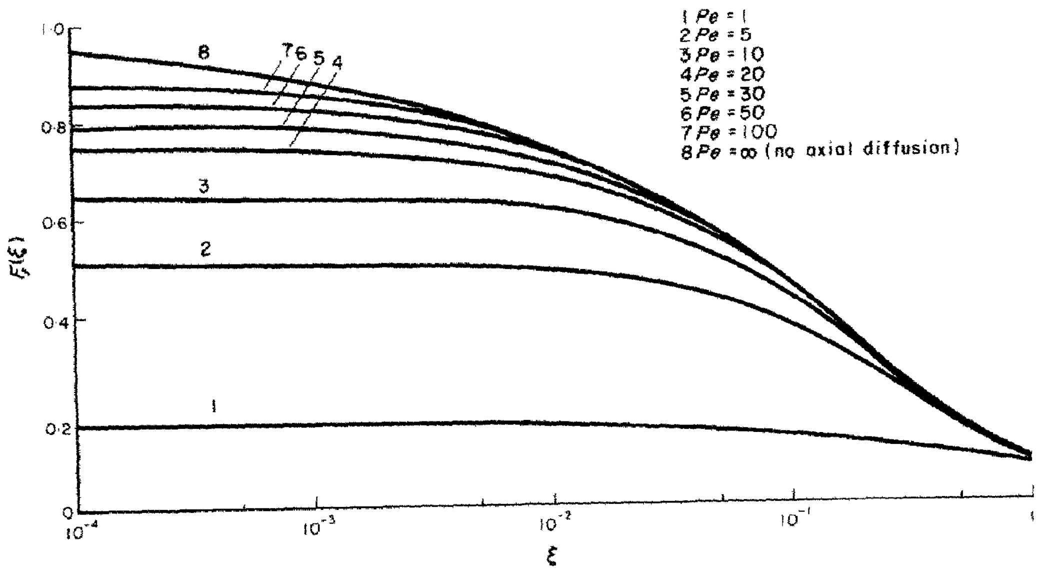

FIG. 10. Variation of $F_f(\xi)$ in the entrance-region of a Poiseuille pipe flow.

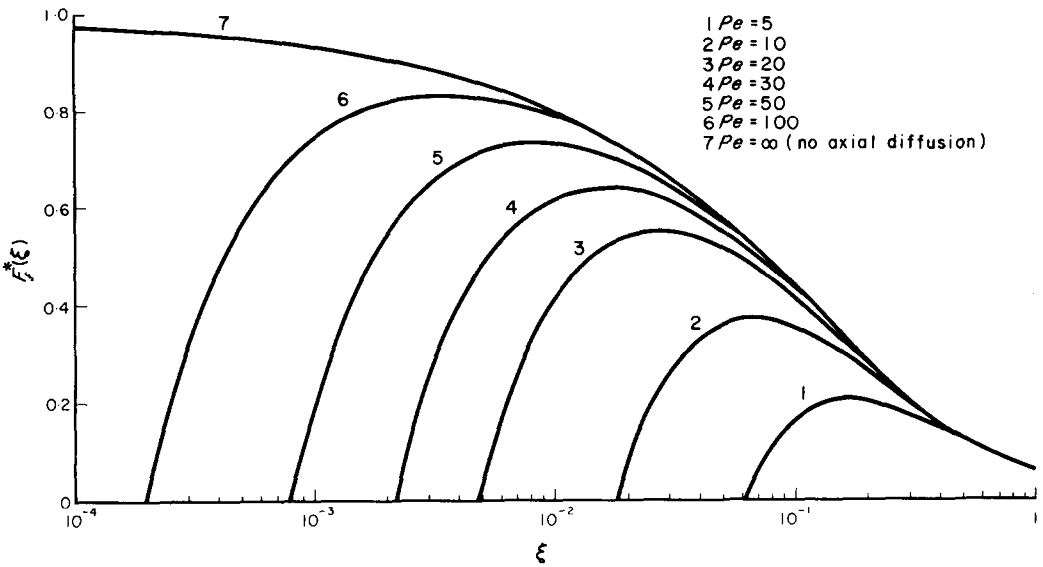

FIG. 11. Variation of $F_f^*(\xi)$ in the entrance-region of a slug flow.

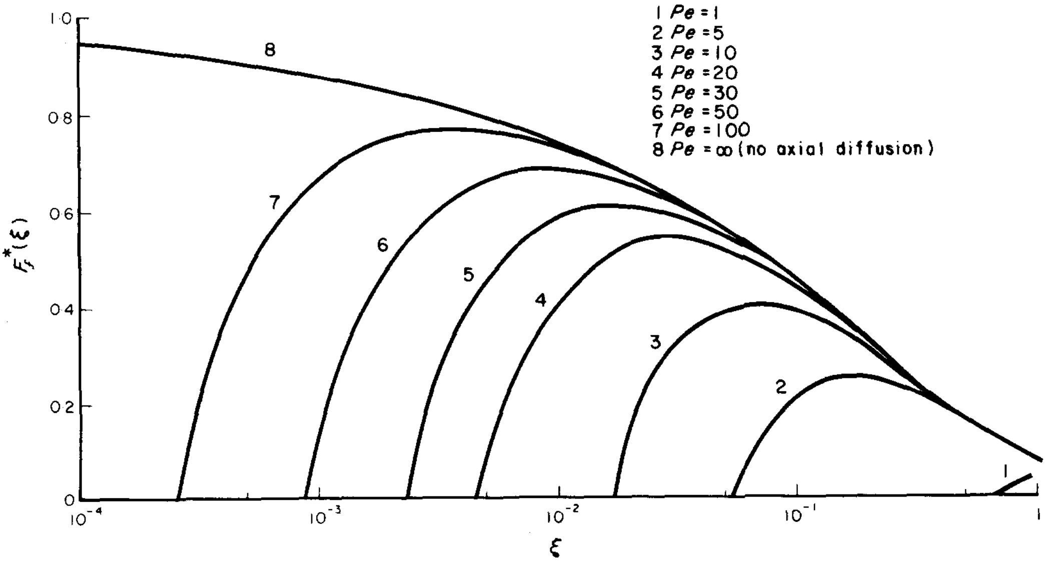

FIG. 12. Variation of $F_f^*(\xi)$ in the entrance-region of a Poiseuille pipe flow.

negative, indicating the upstream-bound axial diffusion flux [i.e. $D(\partial c/\partial x)$] prevails over the downstream-bound convective flux (i.e. $v_x c$). The negative $F_f^*(\xi)$ values are not shown in Fig. 11 and 12 since they do not represent physically meaningful data.

It should be borne in mind, therefore, that in using the $F_f(\xi)$ values, defined by equation (33), in the experimental determination of the coefficient of diffusion, one has neglected the axial diffusive flux which becomes more important as ξ values and *Pe* get smaller. The $F_f(\xi)$ values thus obtained tend to be higher than the actual values whenever axial diffusion plays a role.

REFERENCES

1. C. W. TAN, Diffusion of disintegration products of inert gases in cylindrical tubes, *Int. J. Heat Mass Transfer* **12**, 471–478 (1969).
2. J. W. THOMAS and P. C. LECLARE, A study of the two-filter method for Radon-222, *Health Phys.* **18**, 113–122 (1970).
3. W. M. KAYS, Numerical solutions for laminar-flow heat transfer in circular pipes, *Trans. Am. Soc. Mech. Engrs* **77**, 1265–1274 (1955).
4. P. J. SCHNEIDER, Effect of axial fluid conduction on heat transfer in the entrance region of parallel plates and tubes, *Trans. Am. Am. Soc. Mech. Engrs* **79**, 765–773 (1957).
5. C. J. HSU, An exact mathematical solution for entrance-region laminar heat transfer with axial conduction, *App. Sci. Res.* **17**, 359–376 (1967).
6. S. N. SINGH, Heat transfer by laminar flow in a cylindrical tube, *Appl. Sci. Res.* **7A**, 325–340 (1958).
7. J. R. SELLARS, M. TRIBUS and J. S. KLEIN, Heat transfer to laminar flow in a round tube or flat conduit—the Graetz problem extended, *Trans. Am. Soc. Mech. Engrs* **78**, 441–448 (1956).

TRANSFERT DE MASSE DE PRODUITS EN DÉCOMPOSITION AVEC DIFFUSION AXIALE DANS DES TUBES CYLINDRIQUES

Résumé—Le problème du transfert de masse stationnaire avec diffusion axiale de produits en décomposition résultat de la désintègration d'un gaz inerte dans un tube est considéré pour un écoulement en bloc et du type Poiseuille. Les produits de désintégration sont filtrés vers l'extérieur du tube de gaz inerte le long du tube cylindrique. Les radio-éléments diffusent axiallement et radialement jusqu'aux parois du tube où ils se décomposent en d'autres radio-éléments.

A cause de la dépendance du nombre de Péclét, les effets de la diffusion axiale sur la distribution de concentration, le nombre de Sherwood local, et les valeurs de $F(\xi)$ sont étudiés pour les nombres de Péclét 1, 5, 10, 20, 30, 50 et ∞.

Pour l'écoulement du type Poiseuille, les expressions asymptotiques pour les valeurs propres et $R_n'(1)$ sont ainsi obtenues.

MASSENTRANSPORT ZERFALLENDER PRODUKTE BEI AXIALER DIFFUSION IN ZYLINDRISCHEN ROHREN

Zusammenfassung—Das Problen des Massentransportes im stationären Zustand bei axialer Diffusion zerfallender Produte, wie es sich infolge der Zersetzung eines Inertgases ergibt, wird für eine schleichende Rohrströmung und für eine Poiseuillesche Rohrströmung untersucht. Die Zerfallsprodukte werden längs der zylindrischen Röhre herausgefiltert. Die radioaktiven Elemente diffundieren axial und radial zu den Rohrwänden und zerfallen dort in andere radioaktive Elemente. Aus der Abhängigkeit von der Péclét-zahl kann die Wirkung der axialen Diffusion auf die Konzentrationsverteilung, auf die örtliche Sherwood-zahl und auf die $F(\zeta)$-Werte für Péclét-zahlen von 1, 5, 10, 20, 30, 50 und ∞ ermittelt werden. Für laminare Rohrströmung werden auch asymptotische Ausdrücke für die Eigenwerte und für $R_n'(1)$ erhalten.

МАССООБМЕН ПРОДУКТОВ РАЗЛОЖЕНИЯ ПРИ ОСЕВОЙ ДИФФУЗИИ В ЦИЛИНДРИЧЕСКИХ ТРУБАХ

Аннотация—Рассмотрена задача стационарного массообмена при осевой диффузии продуктов радиоактивного разложения инертного газа при ползучем и пуазейлевском течении. Продукты разложения фильтруются в инертном газе вдоль цилиндрической трубы. Радиоактивные элементы диффундируют по оси и по радиусам к стенкам трубы, где они разлагаются на другие радиоактивные элементы.

Исследуется влияние осевой диффузии на распределение концентрации, локальное число Шервуда и значения $F(\xi)$ для чисел Пекле 1,5, 10, 20, 30, 50 и ∞.

Для пуазейлевского течения в трубах получены асимптотические выражения для собственных значений и $R'_n(1)$.